

Unravelling community assemblages through multi-element stoichiometry in plant leaves and roots across primary successional stages in a glacier retreat area

Yonglei Jiang · Mengya Song · Sheng Zhang ·
Zhiquan Cai · Yanbao Lei

Received: 16 November 2017 / Accepted: 10 May 2018 / Published online: 17 May 2018
© Springer International Publishing AG, part of Springer Nature 2018

Abstract

Background and aims Our understandings on the patterns and mechanisms of plant community assembly during succession, especially the primary succession in glacier retreat areas, remain limited. The *Hailuoguo Glacier Chronosequence* provides a distinctive place to disentangle the biotic interactions and abiotic filtering effects on community successional trajectories.

Methods Through community-weighted approaches, we quantified elements allocation and regulation in leaves and roots, N:P stoichiometry, and the biotic and abiotic controls guiding community dynamics along the 120-year chronosequence.

Results Across seven primary successional stages, plant leaves featured higher concentrations of macro-

elements with lower coefficients of variation (CV) with increasing succession; whereas, fine roots contained more micro-elements with higher CV. From the early to late stages, foliar N:P increased linearly from 8.2 to 20.1.

Conclusions These findings highlighted that the limiting factor for plant growth shifted from N to P over one century of deglaciation. Edaphic factors (pH, bulk density, N and P concentrations) acted as deterministic filtering for trait convergence in the early stages, while biotic factors (species richness and plant litter biomass) for competitive exclusion dominated the late stages hosting species with stronger homeostatic regulation and more conservative nutrient use.

Keywords Edaphic and biotic drivers · *Hailuoguo Glacier Chronosequence* · Elements homeostatic regulation · Plant community assembly

Responsible Editor: Hans Lambers.

Electronic supplementary material The online version of this article (<https://doi.org/10.1007/s11104-018-3683-9>) contains supplementary material, which is available to authorized users.

Y. Jiang · M. Song · S. Zhang · Y. Lei (✉)
Key Laboratory of Mountain Surface Processes and Ecological Regulation, Institute of Mountain Hazards and Environment, Chinese Academy of Sciences, Chengdu 610041, China
e-mail: leiyb@imde.ac.cn

Y. Jiang · M. Song
University of Chinese Academy of Sciences, Beijing 100039, China

Z. Cai
Key Laboratory of Tropical Plant Resources and Sustainable Use, Xishuangbanna Tropical Botanical Garden, Chinese Academy of Sciences, Mengla 666303, China

Introduction

Global warming has caused glacial recessions worldwide since the end of the Little Ice Age (~1850); for example, half of the glaciers retreated in the European Alps, mainly after 1985 (Zemp et al. 2006), and approximately 20% in the Tibetan Plateau due to the 0.23 °C temperature increase per decade during 1951–2009 (Guo et al. 2015). The new ice-free areas following the glacial retreat and colonization by terrestrial organisms provide an opportunity to study primary succession from the very beginning. Plant–soil interactions in these

infertile environments are crucial for understanding the diversity and productivity of plant communities, and ultimately the rate and direction of ecosystem succession (Wardle et al. 2004). Deciphering the patterns and driving agents of successional dynamics in terrestrial ecosystems is one of the major tasks of plant ecology; however, our understandings of how functional traits change across primary successional gradients, especially in deglaciated terrains, are still modest.

Soil nutrient availabilities, particularly nitrogen (N) and phosphorus (P), are important and reliable indicators of ecosystems functioning. Equally important are their stoichiometric balances related to carbon (C), because strict proportions of C, N and P can be deterministic for species interactions, trophic cascades and nutrient recycling (Elser et al. 2007; Yu et al. 2010). Furthermore, homeostatic regulation to maintain a given elemental concentration despite variations in the environment can be highly related to a species' ecological strategy and evolutionary fitness (Jeyasingh et al. 2009). Indeed, Yu et al. (2010) showed that species with strong regulatory capacity are dominant in communities under low nutrients conditions; ecosystems dominated by homeostatic taxa usually exhibit higher productivity. Under stressful conditions, as the maintenance of stoichiometric homeostasis is energetically expensive for plants, higher stoichiometric N:P flexibility might be advantageous, which allows for opportunistic uptake of the remaining nutrients, especially for the subordinate species (Sardans et al. 2015; Mariotte et al. 2017; Sperfeld et al. 2017). Besides the great importance given to soil N and P, many other elements (including macro- and micro-elements) are also indispensable for the proper functioning of plant communities in specific contexts or regions, either due to limitations or toxicity, or impacts on C, N and P cycling (Han et al. 2011). For instance, leaf Mg is strongly correlated with chlorophyll synthesis, plant photosynthesis, and enzyme activation; Ca can improve membrane stability and increase stress tolerance; K and Na act as important determinants of stomatal control and osmoregulation, especially in arid and saline environments; and Mn, Zn, Fe, and Cu are essential for protein synthesis and enzymatic activities (Miatto et al. 2016). The necessity to consider the potential effect and response of multiple elements in plant communities has been given more recognition in terrestrial ecology nowadays (Aerts and Chapin 2000; He et al. 2016; Zhao et al. 2016). Moreover, among the multiple elements, those with high physiological

requirements, high average concentrations and most frequently limiting in nature would be more stable and less sensitive to environmental variations (Han et al. 2011). Thus, new knowledge on the variation of plants' nutritional traits and how tightly bound they are to environmental gradients is critical to the development of a broad (rather than nitrogen-centric) perspective on plant nutritional ecology, and this will help to better parameterize complex multi-element biogeochemical models to forecast community dynamics (Lambers et al. 2008; Han et al. 2011; Sardans et al. 2015).

Despite the facts that diverse patterns of plant stoichiometry with environmental conditions can be found, our understanding on the underlying drivers of variability in stoichiometry, as well as the relative contribution of different community assembly processes, is still in its infancy. Trait-based methods placing species along the quantitative axes of niche partitioning has been shown to be a powerful way of examining the ecological processes involved in the assemblages of tree communities, in which both abiotic conditions and biotic interactions impose deterministic roles on functional trait diversity (Rejou-Mechain et al. 2014; Lohbeck et al. 2015; Botta-Dukát and Czúcz 2016). Abiotic filtering has been suggested to enhance species similarity under more stressful conditions, contributing to low functional diversity among sympatric species (Weiher et al. 2011; Bergholz et al. 2017). In contrast, biotic filtering might generate more complex results, because in stressful environments facilitation can stimulate functional diversity through preventing coexisting species from being too similar; nevertheless, in benign environments, strong competition may decrease functional diversity (Weiher et al. 2011; Bergholz et al. 2017). More studies are critically needed not only for predicting the community successional dynamics, but also for improving management, conservation, and restoration strategies in the disturbed ecosystems.

In this study, using the community-weighted means for the concentration, variance and regulation of eleven elements in leaves and fine roots, we investigated the patterns of primary successional trajectories across a glacier-retreating chronosequence, and the underlying environmental and biological driving forces. We aimed to test the following hypotheses: (1) for macro- and micro-elements, the inconsistent changes in their availabilities and divergent allocations within plant organs (i.e., leaves and fine roots) would result in contrasting patterns for the community-weighted means across the chronosequences in different organs; (2) species with

relatively high nutrient use and flexible nutrient stoichiometry would dominate in early succession, whereas species in later successional stages would be characterized by conservative resource-use strategies and stronger stoichiometric regulation related to higher biomass accumulation; (3) the limiting nutrients for plant growth would gradually shift from N to P over one century of deglaciation; meanwhile, the dominating drivers for community assemblages would transition from edaphic factors under early infertile conditions, to biotic factors under the later productive stages. Our analyses allowed us to uniquely characterize how community-wide functional traits change during the primary succession at a local scale, and to disentangle the effects of biotic interactions and abiotic filtering on the overall plant stoichiometry patterns, and thus could shed new light on the rate, direction and magnitude of ecosystem succession under future global changes.

Materials and methods

Study sites

The *Hailuoguo Glacier Chronosequence*, located on the eastern fringe of the Tibetan Plateau (29°30' to 30°20' N, 101°30' to 102°15' E, 7556 m a.s.l.), has been described in detail by Lei et al. (2015) and Zhou et al. (2016). The relatively mild and humid climate here promotes rapid moraine colonization by plants and microbes (Lei et al. 2015). Spatial differences in the lithology, topography, and climate are negligible in such a small area (<0.5 km²), because of the small gradients in length (2 km), width (50–200 m), elevation (127 m from 2982 to 2855 m) and soil temperature (0.62 °C from 6.06 to 5.44 °C). At this site, several studies have investigated specific processes or organisms, and usually found non-linear changing patterns, such as pedogenesis, weathering processes (Zhou et al. 2016), plant succession (Zhong et al. 1997; Yang et al. 2014) and soil nematodes (Lei et al. 2015). After 120-years of primary succession, the chronosequence has developed into distinct vegetation communities, changing from a pioneer to climax community at seven successional ages (3, 12, 30, 40, 52, 80 and 120 years, respectively) (Fig. S1). The newly deglaciated moraine, after retreating for 3 years, is characterized by N₂-fixing *Astragalus adsurgens* Pall. and *A. souliei* N.D. Simpson. The second stage, after 12 years, is dominated by pioneer trees and shrubs (i.e.

Hippophae rhamnoides L. and *Salix magnifica* Hemsl.) and a few other leguminous herbs. *H. rhamnoides* L., *Salix* spp. and *Populus purdomii* Rehd. are dominant at the third and fourth stage after deglaciation for 30 to 40 years, where competition is likely to be strong due to the high population density. Stage 5 harbors a diverse community including *Betula utilis* D. Don, *P. purdomii*, *Abies fabri* (Mast.) Craib and other shrubs and grasses. After 80 years of development, stage 6 consists of *P. purdomii*, *A. fabri* and *Picea brachytyla* (Franch.) Pritz. The last stage, stage 7, is dominated by the conifers *P. brachytyla* and *A. fabri* (Table S1). Thus, it provides a distinctive opportunity to explore the controls over vegetation succession and soil development (Fig. S1). Along with the forest succession, Yang et al. (2014) found that C:N ratios in mineral soils decreased significantly due to a more rapid N accumulation rate compared with C accumulation.

Field survey and sampling

At each chronosequence stage, in August 2015, we sampled three 10 × 10 m square plots with a distance of 10 m between plots (except stages 1 and 2 with 5 × 5 m square plots and a 3-m distance between plots due to their relatively small areas covered). In each plot, all the taxa of plant communities were listed at species level to assess plant composition and richness (Table S1). Then, five mature, sunlit leaves and the fine roots (diameter < 2 mm) attached to the woody plants were collected from five replicate individuals of each dominant species. For soil samples, as with previous studies here, for the first two sites only fine moraine materials in the top 10 cm could be collected (Zhou et al. 2016). For the other five stages, three soil units were collected to include O, A and C horizons, which represent litter layer, soil with dark brown color and humus enrichment, and soil parent material, respectively. Due to the immaturity of soil development, the boundaries of the three horizons were inconspicuous, and none of the soils showed cambic (B), eluvial (E), or illuvial (Bs, Bh) horizons. Moreover, Zhou et al. (2016) found that the thickest A horizon was only approximately 12 cm thick. Thus, we collected the top soils (10 cm in the first two stages, and 20 cm in the other five stages) from the center and each corner in each plot using a 5-cm diameter soil corer. The five soil cores were combined and homogenized as one composite soil sample, passing through a 2-mm sieve after removing roots. The composite samples were stored in

polyethylene bags and transported to the laboratory. All sampling pits were under canopies of the dominant plants of each stage, not on steep slopes or near small streams within the chronosequence.

Community structure, aboveground and litter biomass measurement

Species frequency and abundance, including the tree, shrub and herb layers was assessed by calculating the total numbers of the species in each plot following the method of Yang et al. (2014). We used the above-ground biomass (Mg ha^{-1}) that had accumulated to represent forest above-ground biomass production. Trees and tall shrubs (higher than 3 m) within the plots were numbered, tagged and measured by height and diameter at breast height (1.3 m above root collar). Their biomass estimates were calculated with the species-specific provincial allometric biomass equations reported by Zhong et al. (1997). For the low shrub and herb layer, the above-ground biomass was estimated by destructively harvesting samples within the central 1×1 m of each subplot. All sampled plant materials were sorted by species, and then were oven-dried at 65 °C for 48 h and weighed for their dry mass. Litter samples were collected using 1-mm mesh litter traps with collection area of 0.42 m², at >0.5 m high from the ground to avoid tidal water. The litter traps were emptied monthly and individual litter components were dried at 80 °C for 48 h, desiccated at room temperature and weighed.

Elemental and isotope composition analyses

The plant leaves and fine roots were cleaned thoroughly with deionized water, oven-dried and ground to a fine powder (250 μm pore size) for total element concentrations analyses. Soil samples were mixed, lightly crushed and air-dried at room temperature, and the large stones, roots, litter and other debris were picked out by sieving through 2-mm plastic sieves. Then, a subsample of the soils was finely milled, passed through a polyethylene sieve of 150 μm pore size before chemical analysis (He et al. 2016). Briefly, 0.5 g plant samples were acidified with 8 ml ultrapure concentrated HNO_3 , and 0.15 g soils were treated with 8 ml ultrapure concentrated mixture of 2.5 ml (HNO_3) + 4 ml (HF) + 1.5 ml (HClO_4) (He et al. 2016). Then all samples were

solubilized in 50 ml Teflon centrifuge tubes and digested in a microwave digestion system (Mars X press Microwave Digestion system, CEM, Matthews, NC, USA) prior to elemental analysis. Blank solutions (acid mixture without samples) were measured in duplicate during each group of sample digestion. To assess the precision and accuracy of the digestions and analytical procedures, we used poplar leaves (GBW 07604) and agricultural soil (GBW E070045) from the China Standard Reference Materials Centre (He et al. 2016). Both plant and soil samples were analysed for total element concentrations of P, K, Ca, Mg, Cu, Na, Mn, Zn, Fe and Al with an inductively coupled plasma optical emission spectroscopy (ICP-OES 7000DV, Perkin Elmer, USA), as described by He et al. (2016). The relative standard deviation for micro- and macro-elements was approximately 1–2%.

In addition, nitrogen concentrations in leaves and roots were measured with a Vario MAX CN element analyzer (Elementar Analysensysteme GmbH, Hanau, Germany). Soil total N was measured by the semimicro-Kjeldahl method. Available N (ammonium and nitrate) concentration was measured after 1 h shaking with 2 M KCl at 1:10 soil extractant ratio. Ammonium-N and nitrate-N was determined as described by Cavagnaro et al. (2006). Available P was extracted by the anion exchange resin and the concentration was determined colorimetrically on a UV-VIS spectrophotometer (Shimadzu UV2450) at 710 nm (Murphy and Riley 1962). For bulk density analysis, soil samples were oven-dried at 105 °C and weighed, then bulk density was calculated by dividing the weight with the sample volume. Soil pH was determined in soil suspensions (soil:water ratio of 1:5) with a potentiometer pH meter (E-INGINST Electron Co., Ltd., Qinxinyang Industrial Zone, Fujian, China) and soil organic carbon content was measured by the dichromate oxidation method (Nelson and Sommers 1982).

Stable carbon ($\delta^{13}\text{C}$) and nitrogen isotope composition ($\delta^{15}\text{N}$) in leaf and fine root samples were measured using a DELTA V Advantage Isotope Ratio Mass Spectrometer (Thermo Fisher Scientific, Inc., Waltham, MA, USA), as described in our previous study (Song et al. 2017). Results are expressed relative to the standard Pee Dee Belemnite as $\delta^{13}\text{C}$ for C and $\delta^{15}\text{N}$ for N stable isotopes in ‰: $\delta^{13}\text{C}$, $\delta^{15}\text{N}$ (‰) = $(R_{\text{sample}}/R_{\text{standard}} - 1) \times 1000$, where R is the $^{13}\text{C}/^{12}\text{C}$ or $^{15}\text{N}/^{14}\text{N}$ ratio, respectively.

Calculation of community-weighted elements stoichiometry

Community-weighted mean values, based on the importance values of the dominant species, are more useful than values based on a single plant species or on the unweighted mean value of many species (Curtis and McIntosh 1951; Niinemets and Kull 2005; Townsend et al. 2007; Zhang et al. 2015). Therefore, the community weighted elements stoichiometry was calculated to determine the community succession across the chronosequence using species importance values in each plot (Skeen 1973; Garnier et al. 2004; Lohbeck et al. 2015), following the three equations:

$$IV_{ik} = (\text{relative abundance} + \text{relative frequency} + \text{relative dominance})/3 \quad (1)$$

$$IV = \sum_{i=1}^n IV_{ik} \quad (2)$$

$$CWM_j = \frac{\sum_{i=1}^n t_{ij} \times IV_{ik}}{IV} \quad (3)$$

Where IV_{ik} is the importance value of species i in plot k , IV is the sum of the IV_{ik} in plot k , n is the number of species in the plot. t_{ij} is the element concentration j of species i in plot k . CWM_j represented the community-weighted means concentration of element j .

The community homeostatic regulation coefficient (R) was calculated according to Sterner and Elser (2002) and Yu et al. (2010):

$$y = cx^{1/R} \quad (4)$$

Where y is the plant community-weighted mean elements content or N:P ratio in leaves or roots, x is the soil element contents or N:P ratio and c is a constant. According to the RDA results, two groups of stages (early S1–5 and late S6–7) could be differentiated; thus, for simplicity the regulation coefficients for early and late stages were calculated separately.

Statistical analyses

Analyses were performed on the means of the community-weighted elemental concentrations of leaves and roots, with the variation quantified by the

coefficient of variation (CV). The relationships between community-weighted mean plant (leaves and roots) elements and stand age were fitted using linear or non-linear regressions. All data were analyzed using SPSS 19.0 for Windows statistical software package (SPSS, Chicago, IL, USA). Community-weighted mean traits among different stand ages were compared by the Tukey's test after one-way ANOVA.

Relationships of community-weighted mean elements between leaves and roots were investigated by model II regression analysis (reduced major axis regression, RMA) with the SMATR package in software R, since both x and y variables included estimation errors (Warton et al. 2012). Allometric relationships between leaves and roots were examined using the scaling approach, $Leaf = a \cdot Root^b$. After log-transformation, the power function was expressed by a linear regression equation, where a and b are the regression intercept and slope, respectively (He et al. 2016); the scaling relationship between leaf and root was considered as isometric when the 95% confidence interval of the slope (b) contained 1 (He et al. 2016). Otherwise the relationship is allometric, that is, foliar elements increase faster than elements in the root when b is above 1, or slower than the root elements when b is below 1 (He et al. 2016). Moreover, to further investigate the effect of the edaphic (soil pH, bulk density, SOM and total contents of elements) and biotic properties (species richness, total above-ground biomass (TAB) and plant litter biomass) on the successional community-weighted elements concentrations, redundancy discriminatory analysis (RDA) was applied using the *rda* function in the *vegan* R package (R Core Team 2013). In addition, before the RDA analysis, a detrended correspondence analysis was performed to confirm that the linear ordination method was appropriate for the analyses (gradient lengths <3). The relative contributions of different explanatory variables including biotic and edaphic factors were calculated by canonical variation partitioning (VPA) using the *varpart* procedure in the R package *vegan* (Oksanen et al. 2016). The significance of the RDA model was tested by *anova.cca* function based on 999 permutations (Oksanen et al. 2016). To visualize the complex relationships between total above-ground biomass accumulation and environmental variables in early and late stages, structural equation modeling (SEM) were used to identify the direct and indirect effects. To simplify the model, we chose those characteristics strongly connected to biomass accumulation, including edaphic factors

(pH, bulk density, soil N and P concentrations), as well as biotic factors (plant richness and litter biomass). All the included edaphic and biotic characteristics were subjected to logarithmic transformation to meet the assumptions of normality. The SEM was conducted with the Amos 17.0 software package (Smallwaters Corporation, Chicago, IL, USA). The criteria for evaluation of structural equation modeling fit, such as the p -values, χ^2 values, the akaike information criterion (AIC), and goodness-of-fit index (GFI) were adopted according to Hooper et al. (2008).

Results

Patterns for elemental concentration, variability and allocation in leaves and fine roots

For soil element concentrations, N showed a unimodal pattern along the chronosequence, with peak values at the intermediate successional stages (stage 5). Gradual decreases were observed in P, Ca, K, Mg, and Mn, and no significant changes for Cu, Na, Fe, Al, and Zn (Fig. S2). Concentrations of N, Na and Mn in leaves and roots, as well as Zn in roots increased, whereas P, Fe, Al, $\delta^{13}\text{C}$ and $\delta^{15}\text{N}$ in leaves and roots, as well as K, Ca and Mg in roots, decreased linearly along the chronosequence. Hump-shaped relationships were fitted for Ca and Mg in leaves. Nevertheless, root Cu as well as foliar K, Ca, Mg, Cu and Zn concentrations showed no general changes (Fig. S3).

The difference between the most and the least abundant element concentrations in community leaves and fine roots was more than three orders of magnitude (Fig. 1). Both allometric and isometric allocation

patterns between leaves and fine roots were found for different elements (Table 1, Fig. 1). According to the RMA regression analysis on community-weighted concentrations of leaves vs fine roots, the slopes of macroelements N, P, Mg, and K, as well as microelements Mn and Zn were significantly larger than 1. In contrast, more Cu, Fe, and Al accumulated in fine roots based on the findings that the slopes of their graphed concentrations were less than 1. Allocations for Ca and Na were not significantly different between leaves and fine roots (Table 1, Fig. 1).

The coefficients of variation (CVs) ranged from 14.9% (P) to 84.6% (Al) in leaves, and from 18.0% (P) to 60.6% (Fe) in fine roots, respectively. For macro-elements, the CVs were generally lower in fine roots than those in leaves, whereas the reverse pattern was found for micro-elements across the chronosequence (Fig. 2a, b). At the community level, the negative relationship between elemental concentrations and their CVs was significant for fine roots (Fig. 2b), and marginally significant for leaves (Fig. 2a).

N and P stoichiometry and multi-elemental equilibrium

The community-weighted mean N:P ratios ranged from 8.2 to 20.1 in leaves, and from 10.5 to 31.0 in fine roots (Fig. 3). For both leaves and fine roots, N:P ratios were comparable in the first three stages, and lower than those of the last four stages, in which N:P ratios increased gradually along with the successional stages (Fig. 3). Furthermore, foliar and fine root N:P ratios were positively correlated with N concentrations, while negatively with P concentrations in soil and community-weighted leaf and root tissues, respectively (Fig. 3).

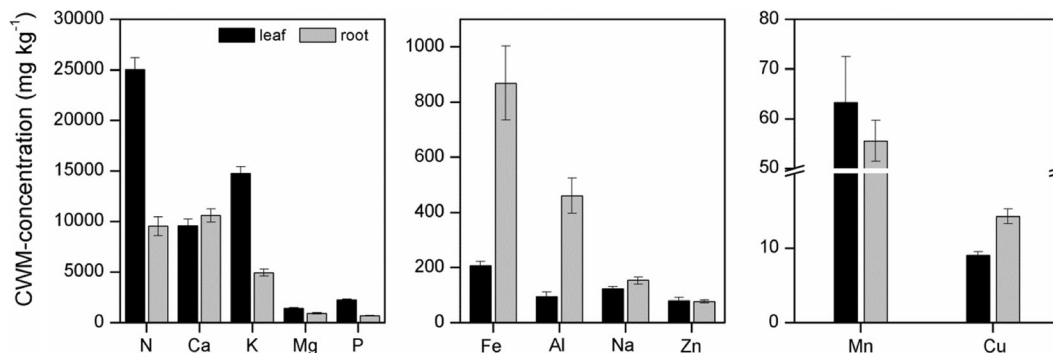


Fig. 1 Community-weighted mean concentrations of the 11 elements in the leaves and fine roots across the seven successional stages in the *Hailuoguo Glacier Chronosequence*

Table 1 Summary of reduced major axis regression on community-weighted mean (CWM) concentrations of 11 elements between leaves and fine roots along the *Hailuoguo Glacier Chronosequence*

Element _{CWM}	RS	95% CI	R ²	P
N	2.06	1.43–2.99	0.38	0.003
P	2.72	1.83–4.03	0.30	<0.001
Mg	1.74	1.21–2.51	0.39	0.003
K	1.81	1.15–2.84	0.86	<0.001
Mn	1.97	1.26–3.10	0.27	0.006
Zn	2.02	1.34–3.03	0.24	0.02
Ca	0.93	0.60–1.44	0.13	0.12
Na	0.91	0.78–1.41	0.25	0.13
Cu	0.41	0.26–0.65	0.44	0.03
Fe	0.28	0.20–0.39	0.49	<0.001
Al	0.28	0.21–0.36	0.74	<0.001

Regression slope (RS) estimates in bold are significantly different from 1 ($P < 0.05$), indicating an allometric relationship existed between leaves and roots. *CI* confidence interval

Ranging from 1.09 to 9.09, the homeostatic regulation coefficients varied according to successional stages, leaf or root organs, and element identities. Across the chronosequence, the late successional stages (i.e., stages 6 and 7) showed higher equilibrium ability than the first five stages, especially for Mg, Ca, Cu, Na, and N:P ratio (Table 2). Homeostatic regulation was higher in leaves than in roots for P, Ca, and N:P, while it was lower for Cu and K, and comparable for other elements. Among these elements, Ca, N, P, and the N:P ratio belonged to

the strong homeostatic ones, but Fe, Al, and Zn exhibited weak homeostatic ability (Table 2).

The relevance of abiotic vs. biotic factors across the chronosequence

Total above-ground biomass increased abruptly in the beginning five stages, and then increased slightly in stages 6 and 7 (Fig. S4 a). Species richness, plant litter and available P increased at the early stages, then maintained at a high level during the last two stages, whereas bulk density exhibited an opposite pattern (Fig. S4 b, c, d and g). A steady increase for inorganic N concentrations was observed, including NH_4^+ and NO_3^- (Fig. S4h).

Based on redundancy analysis (RDA), three clusters were differentiated across the chronosequence, including stage 1 as cluster 1, stages 2–5 as cluster 2, and stages 6–7 as cluster 3. Furthermore, the first two axes of RDA accounted for approximately 51 and 60% of the total variation for leaves' and roots' community-weighted mean elemental concentrations, respectively (Fig. 4a, b). Variation partitioning analysis indicated that, among the environmental factors, pH, soil density, species richness and litter biomass were strongly related to elemental compositions (Table S2; Fig. 4a, b). At the late stages, along with forest establishment the importance of biotic factors as well as the interactions of biotic and edaphic factors increased; meanwhile the explanatory capacity of edaphic factors decreased (Fig. 4c, d). Across the chronosequence, edaphic

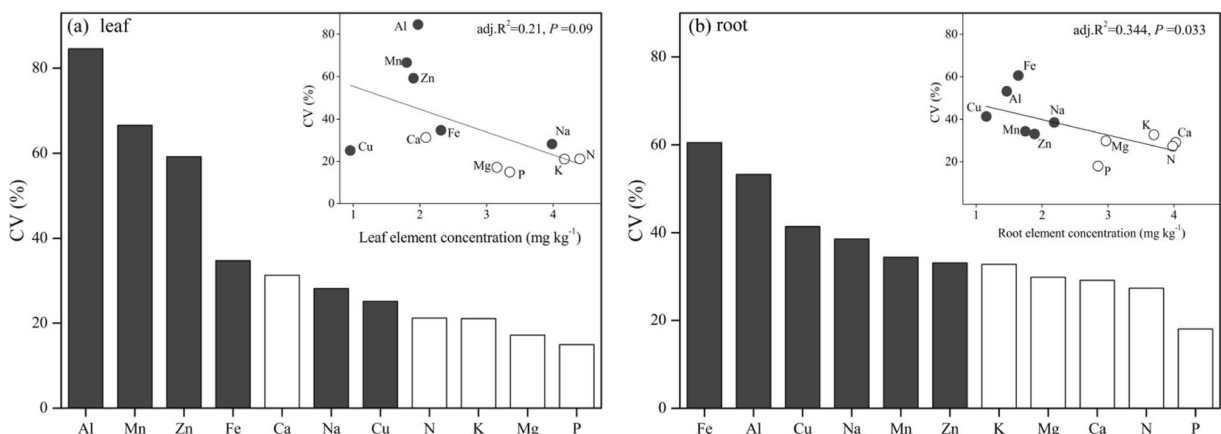


Fig. 2 The coefficient of variation (CV) of elemental concentration in leaves (a) and fine roots (b), and the relationship between elemental concentration and CV. The black and white colored bars represent the micro- and macro-elements, respectively

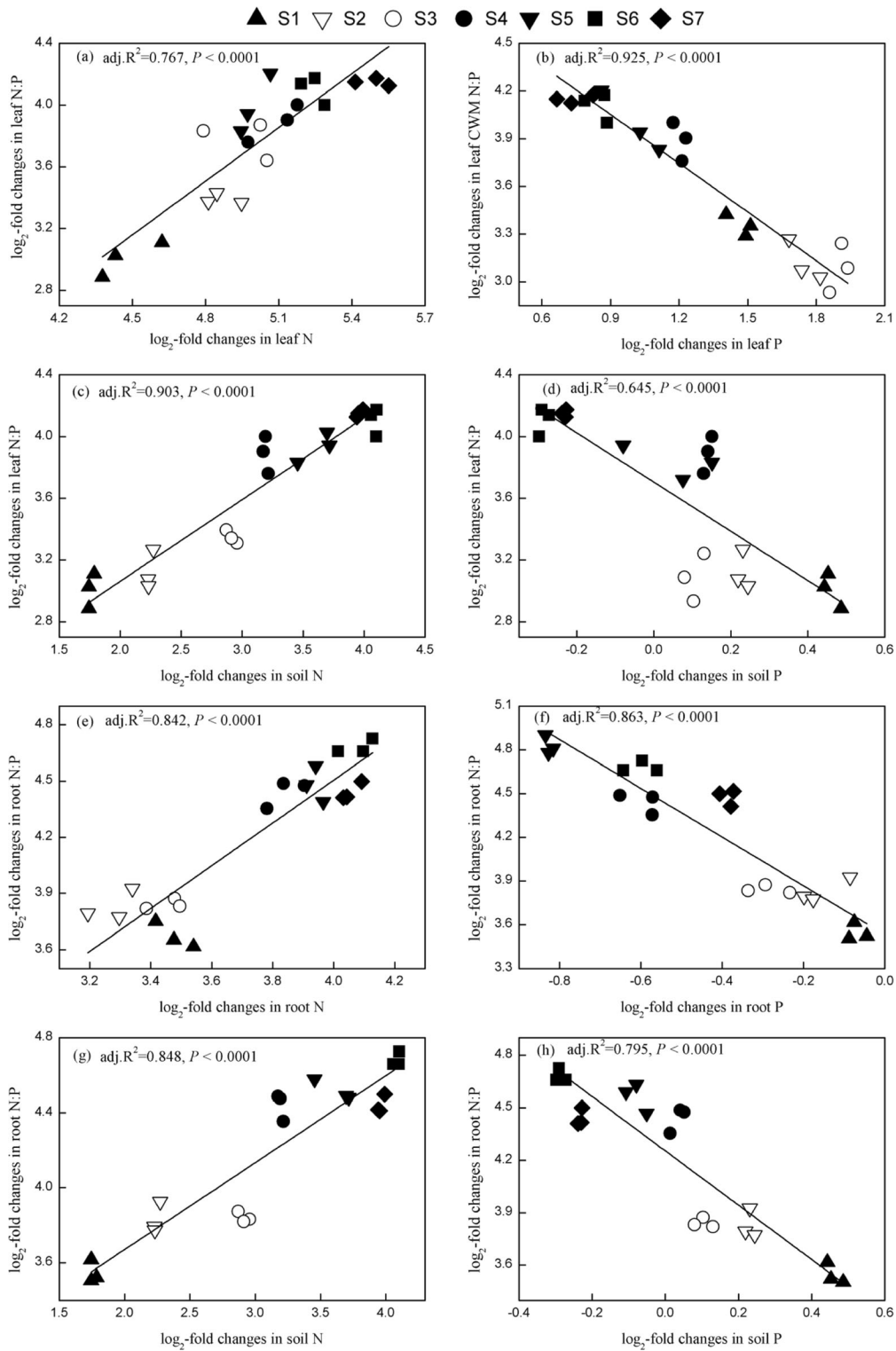


Fig. 3 Correlations between N:P ratios in the leaves or fine roots with log-transformed community-weighted mean concentrations of N and P in leaves and roots, also soil available N and P across

the seven successional stages in the *Hailuoguo Glacier Chronosequence*. The abbreviations S1-S7 represented the seven successional stages of *the Chronosequence*

Table 2 Community-weighted mean (CWM) elements homeostatic regulation coefficients (columns 2–5) in early and late successional stages, and Pearson correlations between leaves and fine roots across the seven successional stages

Elements _{CWM}	Early stages (1–5)		Late stages (6–7)		Leaves vs. Fine roots		
	Leaves	Fine roots	Leaves	Fine roots	Correlation	<i>P</i>	R ²
N	4.74	5.43	4.89	4.54	0.649	0.001	0.665
P	4.01	1.47	4.28	2.94	0.403	0.042	0.453
N:P	4.76	2.77	9.09	5.26	0.529	0.014	0.505
K	2.64	4.76	2.52	3.14	0.237	0.302	0.089
Mg	1.91	1.97	4.30	4.74	0.539	0.012	0.578
Ca	4.31	2.76	5.08	3.88	0.341	0.067	0.277
Mn	1.65	1.61	2.48	1.33	0.321	0.215	0.374
Zn	1.52	1.67	1.69	1.98	0.405	0.037	0.392
Cu	1.35	2.07	2.20	3.00	0.307	0.175	0.186
Al	1.09	2.58	1.88	2.63	0.592	0.005	0.551
Fe	1.29	2.51	1.65	1.68	0.664	0.001	0.501
Na	2.86	1.96	3.52	2.03	0.217	0.323	0.192

and biotic factors explained 10.8 and 25.4% of foliar variation, and 19.5 and 18.0% of roots variation, respectively (Fig. 4c, d). In the SEM models, combining the direct and indirect effects, total absolute effects of environmental factors on above-ground biomass followed the order as soil N (0.83), soil P (0.47), species richness (0.24), pH (0.22), litter biomass (0.18) and soil density (0.10) in the early stages. In the late stages, the order changed to soil N (1.06), soil P (0.84), species richness (0.66), pH (0.37), litter biomass (0.34), and soil density (0.03) (Fig. 4e, f).

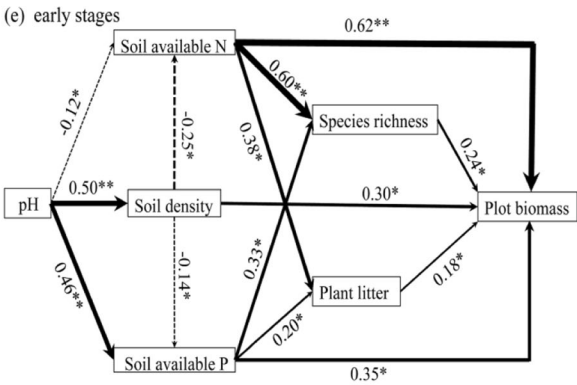
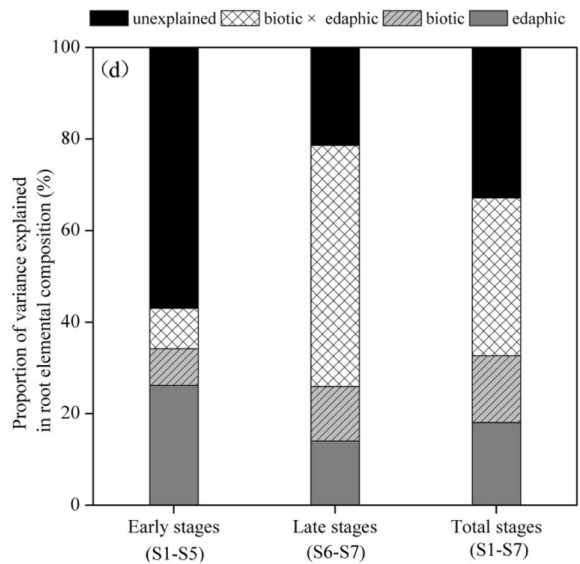
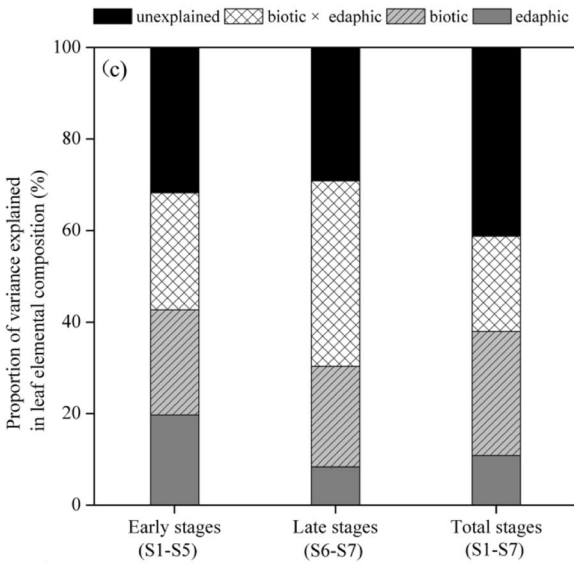
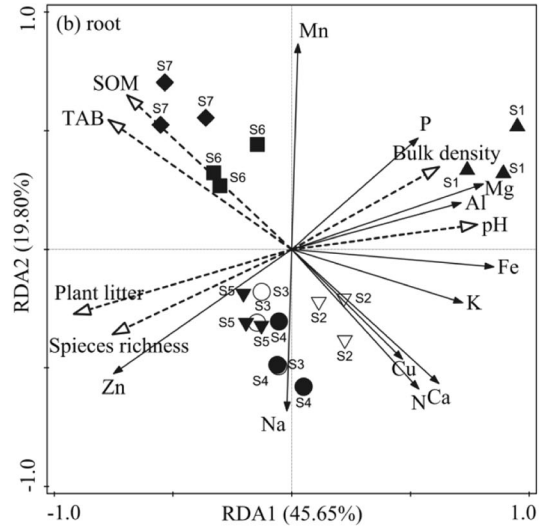
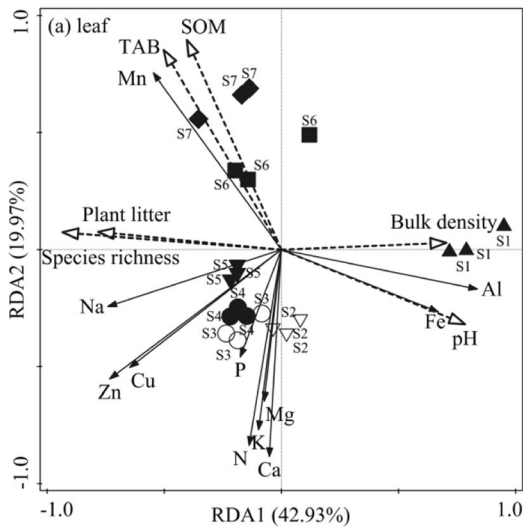
Discussion

Patterns for elemental concentrations, allocations, and homeostatic regulations in leaves and fine roots

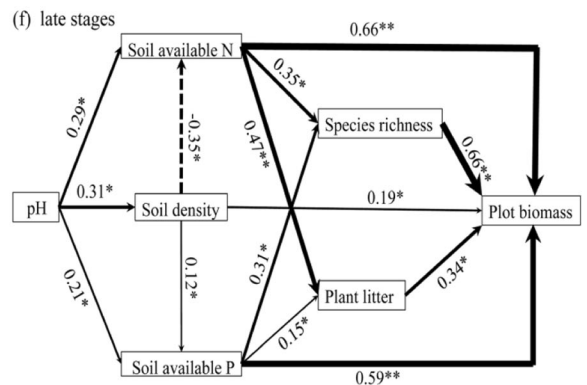
Tissue element concentrations are hypothesized to be relatively resistant to environmental conditions within a species' natural range, and consequently may be deemed as intrinsic functional traits, contributing to the species habitat selection and distribution (Metali et al. 2012). In this study, we found that higher content of macroelements (N, P, K, and Mg) accumulated in the leaves than in the fine roots, whereas fine roots contained more microelements, i.e. Fe, Al, and Cu at the community level across the different successional

stages (Table 1, Fig. 2). These variations of concentrations are likely due to the mobility of those elements in different plant tissues. For example, elements relevant to photosynthesis, including N, P and K, are transported and accumulated in the leaves to enable growth (He et al. 2016; Zhao et al. 2016). In contrast, some trace metals tightly bound within root cells, contributed to a greater accumulation in the belowground parts. Moreover, elements required in higher concentrations during plant development are supposed to be less variable and less sensitive to environmental variation (Han et al. 2011). Indeed, significantly negative relationships were observed between elemental concentrations and their CVs at the community-scale for leaves and fine roots (Fig. 2).

Foliar $\delta^{15}\text{N}$ values, typically an indicator of N cycling rates, as well as overall N availability (Craine et al. 2015), decreased significantly with increasing stand age (Fig. S3m), which was consistent with the results from a temperate rainforest dune chronosequence (Vitousek et al. 2013). The decrease in $\delta^{15}\text{N}$ can be attributed to different N_2 fixation strategies (Vitousek et al. 2013), or shifts in plant composition and competition for nitrogen throughout the succession (Gei and Powers 2013). In our study site, nitrogen-fixing plants (i.e. *Astragalus adsurgens* and *Hippophae rhamnoides*) dominate in the early stages, and their $\delta^{15}\text{N}$ levels usually approach 0‰, reflecting atmospheric isotopic N values (Goodale 2017). At the last two successional stages, the conifers



$\chi^2=15.633$, $df=7$, $p=0.129$, $AIC=33.718$, $GFI=0.911$



$\chi^2=22.627$, $df=7$, $p=0.368$, $AIC=64.628$, $GFI=0.947$

◀ **Fig. 4** Correlations between community-weighted mean concentrations of 11 elements and edaphic and biotic factors were indicated by redundancy discriminatory analysis explained for the percent of total variation (**a, b**) and variation partitioning analysis (**c, d**). The causal relationships of edaphic and biotic variables on total above-ground biomass accumulation were depicted by structural equation modeling (**e, f**). SOM, soil organic matter; TAB, total above-ground biomass. In **e** and **f**, solid and dashed arrows represent positive and negative correlations, respectively. The thickness of the arrows reflects the magnitude of the standardized coefficients. “▲” successional stages 1 (3-years), “▽” successional stages 2 (12-years), “○” successional stages 3 (30-years), “●” successional stages 4 (40-years), “▼” successional stages 5 (52-years), “■” successional stages 6 (80-years), and “◆” successional stages 7 (120-years), respectively

(*Abies fabri* and *Picea brachytyla*) associated with ectomycorrhizal symbiosis for efficient fine root foraging strategies become dominant (Ostonen et al. 2017), which might account for the further reduction in $\delta^{15}\text{N}$ levels.

The regulation coefficients varied with developmental stages, plant organs, and element identities (Table 2). Among variable elements, Ca, N, and P were strongly stable, while Fe, Al, and Zn were weak in equilibrium ability. These findings were similar to the results of Karimi and Folt (2006), who pointed out that homeostatic capacities were highest for macronutrients, intermediate for essential micronutrients and lowest for non-essential metals. Peñuelas et al. (2010) claimed that each species has an optimal elemental composition and stoichiometry for proper functioning in its specific ecological biogeochemical niche, probably within the continuum of the homeostasis–flexibility strategy. Our community homeostatic regulations were also coincident with the vegetation transition from broadleaved shrubs and trees (i.e. *Salix* spp. and *P. purdomii*, faster growing species) to coniferous *A. fabri* and *P. brachytyla* forest (slower growing species) along the primary succession (Lei et al. 2015). Numerous studies have shown that species with high colonization and acquisitive traits would dominate in the early successional stages, whereas later stages would be characterized by species associated with conservative nutrient-use strategies and higher homeostatic capacity (Elser et al. 2007). Strong homeostatic regulation and conservative nutrient use may be critical for species in infertile environments, being important ecophysiological mechanisms to sustain their biomass production and stability (Yu et al. 2010).

N:P stoichiometry and implications for nutrient limitations along the chronosequence

The soil N content increased significantly along with succession and maintained high levels during the latter three stages (Fig. S2 a), resulting from the combination of N_2 fixation and higher litter input (Lei et al. 2015). In contrast, soil P content decreased gradually along the chronosequence (Fig. S2b). Moreover, at the 120 year-old site, the microbial P pool was found to exceed the pool of plant available P, which implied that there was a strong competition between soil microorganisms and plants for P assimilation (Achat et al. 2010; Lei et al. 2015). Along with the variations in soil N and P concentrations, linear increases in N and decreases in P were observed in community weighted means for leaves (Fig. S3a, b). We found that the correlations between foliar and soil available N and P concentrations were not tightly related, probably because some exploitative plants could take up nutritional elements exceeding the minimum requirement, which usually obscured the relationship between plant and environment. The N:P ratio is a powerful index to decipher the mechanisms that couple vegetation structure and function, as well as nutrient limitation (Elser et al. 2007). Generally, a N:P ratio in leaves higher than 16 indicates P limitation at the community level, meanwhile a value of lower than 14 as N limitation; and N:P ratio between 14 and 16 indicates that plant growth is co-limited by both N and P (Tessier and Raynal 2003). Güsewell (2004) provided a more conservative estimate of the N:P ratio threshold values: lower than 10 for N limitation and higher than 20 for P limitation. In our study, the community-weighted mean N:P ratios increased from 8.2 to 20.1 for leaves, and from 10.5 to 31.0 for fine roots, respectively, from the first to the last successional stage (Fig. 3). Moreover, the N:P ratios were positively correlated with N concentrations, while negatively with P in soils and leaves or roots (Fig. 3). Therefore, our results highlighted that the limiting factor for plant growth shifted from N at the early stages to P, as proposed by the classical pedogenesis model (Walker and Syers 1976). At the oldest site, the concentration of bioavailable P was smaller than in any of the younger A horizons, due to the greater requirements for P by *P. brachytyla* and *A. fabri*, their poor litter qualities and the strong competition for P between microorganisms and plants (Fig. S4; Lei et al. 2015). However, increasing foliar N:P ratios with ecosystem development provide only circumstantial evidence for

shifts from N to P limitation, because these ratios are not always reliable indicators for nutrient status and need to be confirmed against results from nutrient-addition experiments (Craine et al. 2008). In our recent work with various types of intra- and interspecific competition between the early successional species *S. rehderiana* and later-appearing species *P. purdomii* under controlled and nitrogen-fertilized conditions, we clearly demonstrated that N plays a pivotal role in determining the asymmetric competition pattern and acts as a key driver for primary succession during the early stages of glacier retreat (Song et al. 2017). Nutrient addition experiments and natural field studies have different benefits and drawbacks, therefore combining both approaches has considerable potential to improve our understanding of nutrient limitation in natural ecosystems.

Driving factors for forest primary successional trajectories in the *Hailuogou Glacier Chronosequence*

At the local scale, soil and microclimate conditions, as well as antagonistic and mutualistic biotic interactions are key factors for species arrival and establishment in primary succession (Arroyo-Rodríguez et al. 2017). In early pedogenic stages, N availabilities were extremely low; therefore, edaphic factors, including pH and soil nutrients, act as deterministic filters resulting in trait convergence (Fig. 4; Pavoine et al. 2011). Similarly, our previous study showed that edaphic properties were the primary agents in shaping microbial community structures at the early stages of this chronosequence (Jiang et al. 2018). In contrast, because of the increased species richness and litter biomass with the establishment of a coniferous forest, the explanatory capacity of biotic factors increased in late stages (stage 6 and 7) for both leaves and roots (Fig. 4), when the soil conditions were not harsh. This pattern was consistent with the Intermediate Disturbance Hypothesis, which states that diversity of competing species is expected to be maximized at intermediate frequencies and/or intensities of disturbance or environmental changes (Callaway et al. 2002). Abiotic conditions do not only affect community structure through environmental filtering, but also through their influence on the outcomes of biotic interactions, with both direction and intensity of interactions changing with environmental gradients (Chamberlain et al. 2014). Therefore, environmental conditions and biotic interactions can interact to produce different trait combinations to drive community assembly. Our results

also highlighted that the high proportions of interacting effects of biotic and abiotic factors played important roles in primary succession in *Hailuogou Glacier Chronosequence* (Fig. 4c, d). Nevertheless, primary succession in glacier retreat areas is a multifactorial phenomenon influenced by a myriad of forces and processes simultaneously operating at multiple spatial and temporal scales (Arroyo-Rodríguez et al. 2017). Future research should integrate novel aspects from current ecological theories to address accurately the patterns and underlying mechanisms for successional trajectories.

Conclusions

In this study, we quantified community-weighted patterns for elemental allocation and regulation in leaves and fine roots, and disentangled the biotic and abiotic drivers guiding the primary successional trajectories along the *Hailuogou Glacier Chronosequence* in the eastern Tibetan Plateau. Plant leaves accumulated higher concentrations of macro-elements (N, P, K, and Mg), with lower coefficients of variation. In contrast, fine roots contained more microelements (Al, Fe, and Cu) with higher variation. The steady increase in leaf N:P ratios, and the respectively positive and negative relationships with N and P suggested that the limiting factor for plant growth shifted from N to P. In early stages where soil nutrient availabilities were low, especially for N, edaphic factors, including pH and soil density would act as deterministic filtering for trait convergence, whereas the explanatory capacity of biotic factors for potentially competitive exclusion increased to dominate in late stages along with the increase in species richness, plant litter biomass and above-ground biomass accumulation. Our results thus can shed new light on the magnitude and direction of ecosystem functioning in future global warming scenarios.

Acknowledgements The authors are grateful to the Gongga Mountain Alpine Ecosystem Observation Station, Chinese Academy of Sciences for logistic support. This work was supported by the National Science Foundation of China (Nos. 31570598 and 31370607), the Talent Program of Hangzhou Normal University (2016QDL020) and the Frontier Science Key Research Programs of Chinese Academy of Sciences (QYZDB-SSW-DQC037). The authors also thank LetPub (www.letpub.com) for its linguistic assistance during the preparation of this manuscript.

References

- Achat DL, Bakker MR, Zeller B, Pellerin S, Bienaimé S, Morel C (2010) Long-term organic phosphorus mineralization in Spodosols under forests and its relation to carbon and nitrogen mineralization. *Soil Biol Biochem* 42(9):1479–1490. <https://doi.org/10.1016/j.soilbio.2010.05.020>
- Aerts R, Chapin FS (2000) The mineral nutrition of wild plants revisited: a re-evaluation of processes and patterns. In: Fitter AH, Raffaelli DG (eds) *Advances in ecological research*, 30, 1–67. [https://doi.org/10.1016/S0065-2504\(08\)60016-1](https://doi.org/10.1016/S0065-2504(08)60016-1)
- Arroyo-Rodríguez V, Melo FPL, Martínez-Ramos M, Bongers F, Chazdon RL, Meave JA, Norden N, Santos BA, Leal IR, Tabarelli M (2017) Multiple successional pathways in human-modified tropical landscapes: new insights from forest succession, forest fragmentation and landscape ecology research. *Biol Rev* 92:326–340. <https://doi.org/10.1111/brv.12231>
- Bergholz K, May F, Giladi I, Ristow M, Ziv Y, Jeltsch F (2017) Environmental heterogeneity drives fine-scale species assembly and functional diversity of annual plants in a semi-arid environment. *Perspec Plant Ecol* 24:138–146. <https://doi.org/10.1016/j.ppees.2017.01.001>
- Botta-Dukát Z, Czúcz B (2016) Testing the ability of functional diversity indices to detect trait convergence and divergence using individual-based simulation. *Methods Ecol Evol* 7: 114–126. <https://doi.org/10.1111/2041-210X.12450>
- Callaway RM, Brooker RW, Choler P, Kikvidze Z, Lortie CJ, Michalet R, Paolini L, Pugnaire FI, Newingham B, Aschehoug ET, Armas C, Kikodze D, Cook BJ (2002) Positive interactions among alpine plants increase with stress. *Nature* 417:844–848. <https://doi.org/10.1038/nature00812>
- Cavagnaro TR, Jackson LE, Six J, Ferris H, Goyal S, Asami D, Scow KM (2006) Arbuscular mycorrhizas, microbial communities, nutrient availability, and soil aggregates in organic tomato production. *Plant Soil* 282:209–225. <https://doi.org/10.1007/s11104-005-5847-7>
- Chamberlain SA, Bronstein JL, Rudgers JA (2014) How context dependent are species interactions? *Ecol Lett* 17:881–890. <https://doi.org/10.1111/ele.12279>
- Craine JM, Morrow C, Stock WD (2008) Nutrient concentration ratios and co-limitation in South African grasslands. *New Phytol* 179:829–836. <https://doi.org/10.1111/j.1469-8137.2008.02513.x>
- Craine JM, Brookshire ENJ, Cramer MD, Hasselquist NJ, Koba K, Marin-Spiotta E, Wang LX (2015) Ecological interpretations of nitrogen isotope ratios of terrestrial plants and soils. *Plant Soil* 396:1–26. <https://doi.org/10.1007/s11104-015-2542-1>
- Curtis JT, McIntosh RP (1951) An upland forest continuum in the prairie-forest border region of Wisconsin. *Ecology* 32:476–496. <https://doi.org/10.2307/1931725>
- Elsler JJ, Bracken MES, Cleland EE, Gruner DS, Harpole WS, Hillebrand H, Ngai JT, Seabloom EW, Shurin JB, Smith JE (2007) Global analysis of nitrogen and phosphorus limitation of primary producers in freshwater, marine and terrestrial ecosystems. *Ecol Lett* 10:1135–1142. <https://doi.org/10.1111/j.1461-0248.2007.01113.x>
- Garnier E, Cortez J, Billès G, Navas ML, Roumet C, Debussche M, Laurent G, Blanchard A, Aubry D, Bellmann A, Neill C, Toussaint JP (2004) Plant functional markers capture ecosystem properties during secondary succession. *Ecology* 85: 2630–2637. <https://doi.org/10.1890/03-0799>
- Gei MG, Powers JS (2013) Do legumes and non-legumes tree species affect soil properties in unmanaged forests and plantations in Costa Rican dry forests? *Soil Biol Biochem* 57: 264–272. <https://doi.org/10.1016/j.soilbio.2012.09.013>
- Goodale C (2017) Multiyear fate of a ¹⁵N tracer in a mixed deciduous forest: retention, redistribution, and differences by mycorrhizal association. *Glob Chang Biol* 23:867–880. <https://doi.org/10.1111/gcb.13483>
- Guo WQ, Liu SY, Xu JL, Wu LZ, Shanguan DH, Yao XJ, Wei JF, Bao WJ, Yu PC, Liu Q, Jiang ZL (2015) The second Chinese glacier inventory: data, methods and results. *J Glaciol* 61: 357–372. <https://doi.org/10.3189/2015JoG14J209>
- Güsewell S (2004) N:P ratios in terrestrial plants: variation and functional significance. *New Phytol* 164:243–266. <https://doi.org/10.1111/j.1469-8137.2004.01192.x>
- Han W, Fang J, Reich PB, Ian Woodward F, Wang Z (2011) Biogeography and variability of eleven mineral elements in plant leaves across gradients of climate, soil and plant functional type in China. *Ecol Lett* 14:788–796. <https://doi.org/10.1111/j.1461-0248.2011.01641.x>
- He M, Dijkstra FA, Zhang K, Tan H, Zhao Y, Li X (2016) Influence of life form, taxonomy, climate, and soil properties on shoot and root concentrations of 11 elements in herbaceous plants in a temperate desert. *Plant Soil* 398:339–350. <https://doi.org/10.1007/s11104-015-2669-0>
- Hooper D, Coughlan J, Mullen M (2008) Structural equation modelling: guidelines for determining model fit. *Electron J Bus Res Methods* 6:53–60
- Jeyasingh PD, Weider LJ, Sterner RW (2009) Genetically-based trade-offs in response to stoichiometric food quality influence competition in a keystone aquatic herbivore. *Ecol Lett* 12:1229–1237. <https://doi.org/10.1111/j.1461-0248.2009.01368.x>
- Jiang Y, Lei Y, Yang Y, Korpelainen H, Niinemets Ü, Li C (2018) Divergent assemblage patterns and driving forces for bacterial and fungal communities along a glacier forefield chronosequence. *Soil Biol Biochem* 118:207–216. <https://doi.org/10.1016/j.soilbio.2017.12.019>
- Karimi R, Folt CL (2006) Beyond macronutrients: element variability and multielement stoichiometry in freshwater invertebrates. *Ecol Lett* 9:1273–1283. <https://doi.org/10.1111/j.1461-0248.2006.00979.x>
- Lambers H, Raven JA, Shaver GR, Smith SE (2008) Plant nutrient acquisition strategies change with soil age. *Trends Ecol Evol* 23:95–103. <https://doi.org/10.1016/j.tree.2007.10.008>
- Lei Y, Zhou J, Xiao H, Duan B, Wu Y, Korpelainen H, Li C (2015) Soil nematode assemblages as bioindicators of primary succession along a 120-year-old chronosequence on the Hailuoguo Glacier forefield, SW China. *Soil Biol Biochem* 88:362–371. <https://doi.org/10.1016/j.soilbio.2015.06.013>
- Lohbeck M, Poorter L, MartiNez-Ramos M, Bongers F (2015) Biomass is the main driver of changes in ecosystem process

- rates during tropical forest succession. *Ecology* 96:1242–1252. <https://doi.org/10.1890/14-0472.1>
- Mariotte P, Canarini A, Dijkstra FA (2017) Stoichiometric N:P flexibility and mycorrhizal symbiosis favour plant resistance against drought. *J Ecol* 105:958–967. <https://doi.org/10.1111/1365-2745.12731>
- Metali F, Salim KA, Burslem DFRP (2012) Evidence of foliar aluminium accumulation in local, regional and global datasets of wild plants. *New Phytol* 193:637–649. <https://doi.org/10.1111/j.1469-8137.2011.03965.x>
- Miatto RC, Wright IJ, Batalha MA (2016) Relationships between soil nutrient status and nutrient-related leaf traits in Brazilian cerrado and seasonal forest communities. *Plant Soil* 404:13–33. <https://doi.org/10.1007/s11104-016-2796-2>
- Murphy J, Riley JP (1962) A modified single solution method for the determination of phosphate in natural waters. *Anal Chim Acta* 27:31–66
- Nelson DW, Sommers LE (1982) Total carbon, organic carbon and organic matter. In: Page AL, Miller RH, Keeney DR (eds) *Methods of soil analysis*. American Society of Agronomy, Madison, pp 539–579
- Niinemets U, Kull K (2005) Co-limitation of plant primary productivity by nitrogen and phosphorus in a species-rich wooded meadow on calcareous soils. *Acta Oecol* 28:345–356. <https://doi.org/10.1016/j.actao.2005.06.003>
- Oksanen J, Blanchet FG, Friendly M, Kindt R, Legendre P, McGinn D, Minchin PR, O'Hara RB, Simpson GL, Solymos PS, Stevens MH, Szoecs E, Wagner H (2016) Package 'vegan'. <http://vegan.r-forge.r-project.org/>
- Ostonen I, Truu M, Helmisaaari H, Lukac M, Borken W, Vanguelova E, Godbold DL, Lohmus K, Zang U, Tedersoo L, Preem JK, Rosenthal K, Aosaar J, Armolaitis K, Frey J, Kabral N, Kukumägi M, Leppälammil-Kujansuu J, Lindroos AJ, Merilä P, Napa U, Njöd P, Parts K, Uri V, Varik M, Truu J (2017) Adaptive root foraging strategies along a boreal-temperate forest gradient. *New Phytol* 215:977–991. <https://doi.org/10.1111/nph.14643>
- Pavoine S, Vela E, Gachet S, de Belair G, Bonsall MB (2011) Linking patterns in phylogeny, traits, abiotic variables and space: a novel approach to linking environmental filtering and plant community assembly. *J Ecol* 99:165–175. <https://doi.org/10.1111/j.1365-2745.2010.01743.x>
- Peñuelas J, Sardans J, Llusia Owen S, Carnicer J, Giambelluca TW, Rezende EL, Waite M, Niinemets Ü (2010) Faster returns on leaf economics and different biogeochemical niche in invasive compared with native plant species. *Glob Chang Biol* 16:2171–2185. <https://doi.org/10.1111/j.1365-2486.2009.02054.x>
- R Core Team (2013) R: a language and environment for statistical computing. R foundation for statistical computing. <http://www.r-project.org>
- Rejou-Mechain M, Flores O, Pelissier R, Fayolle A, Fauvet N, Gourlet-Fleury S (2014) Tropical tree assembly depends on the interactions between successional and soil filtering processes. *Glob Ecol Biogeogr* 23:1440–1449. <https://doi.org/10.1111/geb.12222>
- Sardans J, Janssens IA, Alonso R, Veresoglou SD, Rillig MC, Sanders TGM, Carnicer J, Filella I, Farré-Armengol G, Peñuelas J (2015) Foliar elemental composition of European forest tree species associated with evolutionary traits and present environmental and competitive conditions. *Glob Ecol Biogeogr* 24:240–255. <https://doi.org/10.1111/geb.12253>
- Skeen JN (1973) An extension of the concept of importance value in analyzing forest communities. *Ecology* 54:655–656. <https://doi.org/10.2307/1935356>
- Song M, Yu L, Jiang Y, Lei Y, Korpelainen H, Niinemets Ü, Li C (2017) Nitrogen-controlled intra- and interspecific competition between *Populus purdomii* and *Salix rehderiana* drive primary succession in the Gongga Mountain glacier retreat area. *Tree Physiol* 37:799–814. <https://doi.org/10.1093/treephys/tpx017>
- Sperfeld E, Wagner ND, Halvorson HM, Malishev M, Raubenheimer D (2017) Bridging ecological stoichiometry and nutritional geometry with homeostasis concepts and integrative models of organism nutrition. *Funct Ecol* 31:286–296. <https://doi.org/10.1111/1365-2435.12707>
- Sterner RW, Elser JJ (2002) *Ecological stoichiometry: the biology of elements from molecules to the biosphere*. Princeton University Press, Princeton
- Tessier JT, Raynal DJ (2003) Use of nitrogen to phosphorus ratios in plant tissue as an indicator of nutrient limitation and nitrogen saturation. *J Appl Ecol* 40:523–534. <https://doi.org/10.1046/j.1365-2664.2003.00820.x>
- Townsend AR, Cleveland CC, Asner GP, Bustamante MMC (2007) Controls over foliar N:P ratios in tropical rain forests. *Ecology* 88:107–118. [https://doi.org/10.1890/0012-9658\(2007\)88\[107:COFNRI\]2.0.CO;2](https://doi.org/10.1890/0012-9658(2007)88[107:COFNRI]2.0.CO;2)
- Vitousek PM, Menge DNL, Reed SC, Cleveland CC (2013) Biological nitrogen fixation: rates, patterns and ecological controls in terrestrial ecosystems. *Philos Trans R Soc B* 368:20130119. <https://doi.org/10.1098/rstb.2013.0119>
- Walker TW, Syers JK (1976) The fate of phosphorus during pedogenesis. *Geoderma* 15:1–19. [https://doi.org/10.1016/0016-7061\(76\)90066-5](https://doi.org/10.1016/0016-7061(76)90066-5)
- Wardle DA, Walker LR, Bardgett RD (2004) Ecosystem properties and forest decline in contrasting long-term chronosequences. *Science* 305:509–513. <https://doi.org/10.1126/science.1098778>
- Warton DI, Duursma RA, Falster DS, Taskinen S (2012) SMATR 3—an R package for estimation and inference about allometric lines. *Methods Ecol Evol* 3:257–259. <https://doi.org/10.1111/j.2041-210X.2011.00153.x>
- Weihel E, Freund D, Bunton T, Stefanski A, Lee T, Bentivenga S (2011) Advances, challenges and a developing synthesis of ecological community assembly theory. *Philos Trans R Soc B* 366:2403–2413. <https://doi.org/10.1098/rstb.2011.0056>
- Yang Y, Wang G, Shen H, Yang Y, Cui H, Liu Q (2014) Dynamics of carbon and nitrogen accumulation and C:N stoichiometry in a deciduous broadleaf forest of deglaciated terrain in the eastern Tibetan plateau. *For Ecol Manag* 312:10–18. <https://doi.org/10.1016/j.foreco.2013.10.028>
- Yu Q, Chen Q, Elser JJ, He N, Wu H, Zhang G, Wu J, Bai Y, Han X (2010) Linking stoichiometric homeostasis with ecosystem structure, functioning and stability. *Ecol Lett* 13:1390–1399. <https://doi.org/10.1111/j.1461-0248.2010.01532.x>

- Zemp M, Haeberli W, Hoelzle M, Paul F (2006) Alpine glaciers to disappear within decades? *Geophys Res Lett* 33:L13504. <https://doi.org/10.1029/2006GL026319>
- Zhang W, Zhao J, Pan F, Li D, Chen H, Wang K (2015) Changes in nitrogen and phosphorus limitation during secondary succession in a karst region in southwest China. *Plant Soil* 391:77–91. <https://doi.org/10.1007/s11104-015-2406-8>
- Zhao N, Yu GR, He NP, Wang QF, Guo DL, Zhang XY, Wang RL, Xu ZW, Jiao CC, Li NN, Jia YL (2016) Coordinated pattern of multi-element variability in leaves and roots across Chinese forest biomes. *Glob Ecol Biogeogr* 25:359–367. <https://doi.org/10.1111/geb.12427>
- Zhong XH, Luo J, Wu N (1997) Researches of the forest ecosystems on Gongga Mountain. Chengdu University of Science and Technology Press, Chengdu
- Zhou J, Bing H, Wu Y, Yang Z, Wang J, Sun H, Luo J, Liang H (2016) Rapid weathering processes of a 120-year-old chronosequence in the Hailuoguo Glacier foreland, Mt. Gongga, SW China. *Geoderma* 267:78–91. <https://doi.org/10.1016/j.geoderma.2015.12.024>